SLAC-PUB-9633
January 2003

Frequency Chirped SASE FEL*

S. Krinsky[1] and Z. Huang
Stanford Linear Accelerator Center, Stanford, CA 94309

Abstract

We present a statistical analysis of the temporal and spectral properties of SASE radiation from an energy-chirped electron beam passing through a long undulator. It is found that the coherence time is independent of the chirp, while the range of spectral coherence is linearly proportional to it. We consider the use of a monochromator to pick out a small temporal slice of the radiation output. For the filtered radiation pulse, we determine the pulse duration, the number of modes and the energy fluctuation. We apply our analysis to schemes proposed to generate short x-ray pulses at the LCLS.

Submitted to: Physical Review ST-AB

[1] Permanent address: Brookhaven National Laboratory, Upton, NY 11973

* Work supported by Department of Energy contracts DE–AC03–76SF00515 and DE-AC02-98CH10886.

I. INTRODUCTION

Single pass free-electron lasers (FELs) based on self-amplified spontaneous-emission (SASE) are being developed as sources of high-brightness short-wavelength radiation. In particular, an x-ray SASE FEL, the LCLS [1], is under design at SLAC. Achieving very short (femtosecond) pulse duration is critical to facilitating important areas of scientific research at this facility. Generating short pulses by frequency chirping FEL output has been discussed [2-4], and recently such a scheme has been proposed [5,6] to produce short pulses at the LCLS. The idea is to send an energy-chirped electron beam through the long LCLS undulator to produce frequency chirped output. A monochromator is then used to select a narrow bandwidth. Since the radiated frequency is correlated with the temporal position along the pulse, a short segment of the original radiation is transmitted. This idea can be applied in two ways: (1) in the single-stage approach, the saturated chirped output from the full undulator is monochromated and the filtered radiation is transmitted to the experiment; (2) in the two-stage approach, the unsaturated chirped radiation from a first section of the undulator is extracted and used as a seed in the second section, where it is amplified to saturation by its interaction with the electron beam.

In a recent LEUTL experiment at Argonne National Laboratory [7], properties of chirped SASE were studied using the frequency-resolved optical gating (FROG) technique. It was observed that the spikes in the SASE output have a positive frequency chirp even in the absence of an energy chirp in the electron beam. It was also confirmed that an electron energy chirp mapped directly into the frequency chirp of the FEL output, and under proper conditions the two chirps were made to cancel each other within a spike.

In this paper, we use the one-dimensional FEL equations (neglecting dependence on transverse coordinates) to analyze the temporal and spectral properties of unsaturated frequency-chirped SASE generated by an energy-chirped electron beam. We characterize the statistical properties of the radiation, determining the coherence time and the range of spectral coherence. For the filtered radiation at the exit of a monochromator, we determine the pulse duration, the coherence time and the pulse energy fluctuation. The rms pulse duration σ_t after a monochromator with rms bandpass σ_m is found to be given by

$$\sigma_t^2 = \frac{\sigma_\omega^2 + \sigma_m^2}{u^2} + \frac{1}{4\sigma_m^2}, \tag{1.1}$$

where $u = \Delta\omega / \Delta t$ is the frequency chirp and σ_ω is the rms SASE bandwidth. This result extends that of refs. [5,6] by including the dependence on the SASE bandwidth σ_ω, which limits the minimum duration that can be achieved for a given electron energy chirp. Before saturation σ_ω decreases as the electon beam travels along the undulator. Therefore shorter pulse duration can be obtained further downstream. In Fig. 1, we show the dependence of the pulse duration on the monochromator bandpass and the electron energy chirp near saturation where the SASE bandwidth is minimum. The results presented in this paper will be important for frequency chirped SASE FELs and for schemes using a monochromator to reduce the output pulse duration.

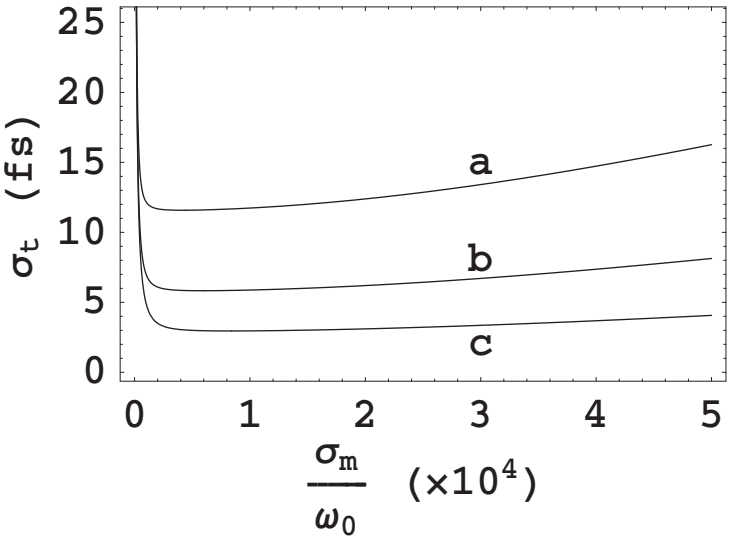

Fig. 1. For LCLS, we plot the rms pulse duration σ_t of the 1.5 $\overset{o}{A}$ $\left(\omega_0 = 1.2\times10^{19}\, s^{-1}\right)$ radiation after a monochromator with rms bandpass σ_m / ω_0 for a (full) energy chirp across the 230 fs electron bunch of: (a) 0.5% as considered in refs. [5,6]; (b) 1% as considered in the LCLS conceptual design report [1]; and (c) 2%. The SASE gain bandwidth is taken to be $\sigma_\omega / \omega_0 = 5\times10^{-4}$, which is the value (equal to the Pierce parameter) expected near saturation.

II. CHARACTERISTICS OF FREQUENCY CHIRPED SASE

Consider an electron beam passing through an undulator having period $\lambda_w = 2\pi / k_w$ and rms field strength parameter a_w. The j^{th} electron has energy γ_j (in units of its rest mass), average longitudinal velocity $v_j \cong c\left(1 - \frac{1+a_w^2}{2\gamma_j^2}\right)$, and arrives at the undulator entrance at time t_j. In the forward direction, the spontaneous radiated electric field has the form

$$E(z,t) \propto \sum_j e^{ik_j z - i\omega_j (t - t_j)} S_j(z, t - t_j), \tag{2.1}$$

where the wave number of the radiation from the j^{th} electron is

$$k_j = \frac{\omega_j}{c} = k_w \left(\frac{v_j}{c - v_j}\right) \cong \frac{2\gamma_j^2 k_w}{1 + a_w^2}, \tag{2.2}$$

and the envelope function S_j is given by

$$\begin{aligned} S_j(z, t - t_j) &= 1, \quad \frac{z}{c} < t - t_j < \frac{z}{v_j}, \\ &= \frac{1}{2}, \quad t - t_j = \frac{z}{v_j}, \\ &= 0, \quad \textit{otherwise.} \end{aligned} \tag{2.3}$$

In this paper, we shall suppose the electron beam energy to have a linear chirp α specified by [5,6]

$$\frac{\gamma_j - \gamma_0}{\gamma_0} = \alpha \frac{t_j}{T_b}, \tag{2.4}$$

where T_b is the full temporal width of the uniform density electron pulse and ct_j is the longitudinal deviation from the beam center $t_j = 0$. From Eq. (2.2), we see that the energy chirp gives rise to a linear frequency chirp

$$\omega_j = \omega_0 + u t_j, \tag{2.5}$$

where $u = 2\alpha\omega_0 / T_b$.

In the exponential growth regime before saturation, the SASE electric field has the form

$$E(z,t) \propto \sum_j e^{ik_j z - i\omega_j (t-t_j)} g(z, t-t_j; u), \tag{2.6}$$

where the green's function can be approximated by (see Appendix A),

$$g(z, t-t_j; u) \cong e^{\rho(\sqrt{3}+i)k_w z} e^{-b\left(t-t_j-\frac{z}{v_g}\right)^2} e^{-\frac{iu}{2}\left(t-t_j-\frac{z}{v_0}\right)\left(t-t_j-\frac{z}{c}\right)}. \tag{2.7}$$

We are ignoring the small reduction in gain [5,6] which enters in $O(u^2)$. In Eq. (2.7), ρ is the Pierce parameter and σ_ω is the SASE gain bandwidth,

$$\sigma_\omega^2 = \frac{3\sqrt{3}}{k_w z}\rho\omega_0^2. \tag{2.8}$$

The complex parameter b is defined by

$$b = \frac{3}{4}\left(1+\frac{i}{\sqrt{3}}\right)\sigma_\omega^2. \tag{2.9}$$

The group velocity is $v_g = \dfrac{\omega_0}{k_0 + \frac{2}{3}k_w}$ and the electron velocity corresponding to energy $\gamma = \gamma_0$ is $v_0 = \omega_0/(k_0 + k_w)$.

In the case of spontaneous radiation, the j^{th} electron emits a wave packet of frequency $\omega_j = \omega_0 + ut_j$, as exhibited in the phase factor in Eq. (2.1). This gives rise to an overall frequency chirp of the output radiation. The individual wave packets are not chirped, since in spontaneous radiation each electron radiates independently and is unaffected by the difference in energy of its neighbors. See Fig.2. In the case of SASE, there is again the dependence of frequency on arrival time, $\omega_j = \omega_0 + ut_j$, as expressed in the phase factor in Eq. (2.6). This results from the dependence of frequency on energy of the initial spontaneous radiation emitted early in the undulator which is amplified in SASE. In addition, the frequency chirp in SASE also appears in the green's function of Eq. (2.7), since the gain process depends both on the emitting electron and those electrons located one slippage distance ahead of it. In fact, the imaginary part of the

parameter b in Eq. (2.9) gives rise to a frequency chirp of the SASE wave packet associated with each electron, even in the absence of an energy chirp of the electron beam, as observed in ref. [7]. See Fig.3.

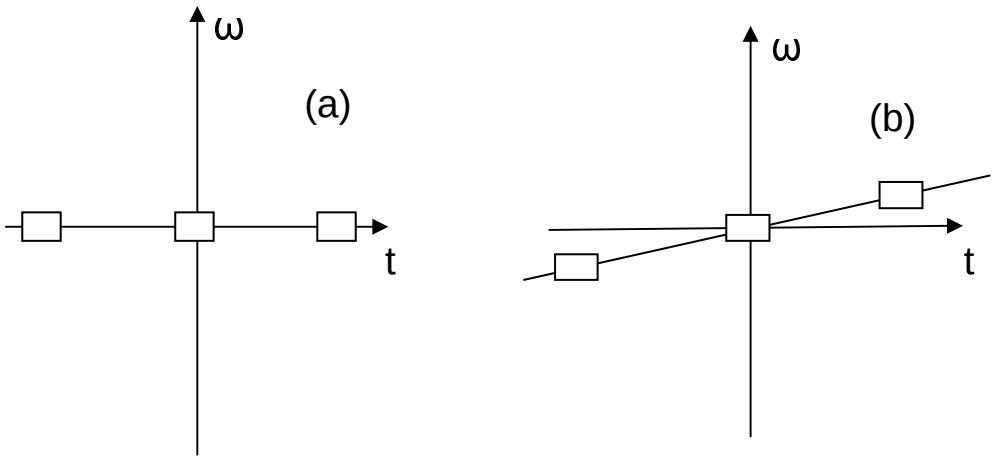

Fig. 2. Time-frequency phase space for: (a) spontaneous radiation with no electron energy chirp; and (b) spontaneous radiation with positive electron energy chirp. The little rectangles correspond to the wave packets emitted by three representative electrons.

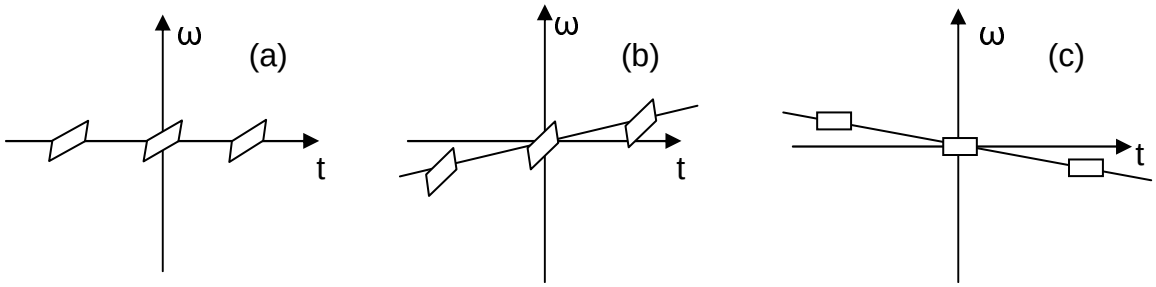

Fig. 3. Time-frequency phase space for SASE with: (a) no electron energy chirp; (b) positive electron energy chirp; (c) negative energy electron chirp chosen to cancel intrinsic SASE frequency chirp as in ref.[7]. The little rectangles represent the wave packets associated with three representative electrons.

To analyze the statistical properties of the chirped SASE output, we consider the arrival times t_j to be random variables and average over the stochastic ensemble [8-10]. We find the time correlation function is given by (see Appendix B)

$$\left\langle E\left(z,t-\frac{\tau}{2}\right)E^*\left(z,t+\frac{\tau}{2}\right)\right\rangle \propto e^{2\rho\sqrt{3}k_w z}\, e^{\frac{-iu\tau}{2}\left(\frac{z}{v_0}+\frac{z}{c}\right)} e^{i(\omega_0+ut)\tau}\, e^{-\sigma_\omega^2\tau^2/2}, \tag{2.10}$$

and the coherence time [8-10]

$$\tau_{coh}=\int d\tau\left|\frac{\left\langle E\left(z,t-\frac{\tau}{2}\right)E^*\left(z,t+\frac{\tau}{2}\right)\right\rangle}{\left\langle\left|E(z,t)\right|^2\right\rangle}\right|^2=\int d\tau e^{-\sigma_\omega^2\tau^2/2}=\frac{\sqrt{\pi}}{\sigma_\omega}. \tag{2.11}$$

Note that the coherence time is given by the inverse of the SASE gain bandwidth, independent of the electron energy chirp.

The frequency correlation function can be determined in terms of the time correlation function according to

$$\left\langle \tilde{E}(z,\omega)\tilde{E}^*(z,\omega+\Omega)\right\rangle=\int dt e^{i\omega t}\int d\tau\, e^{-i(\omega+\Omega)(t+\tau)}\left\langle E(z,t)E^*(z,t+\tau)\right\rangle, \tag{2.12}$$

and using Eq. (2.10) one finds

$$\left\langle \tilde{E}\left(z,\omega-\frac{\Omega}{2}\right)\tilde{E}^*\left(z,\omega+\frac{\Omega}{2}\right)\right\rangle \propto e^{2\rho\sqrt{3}k_w z}\, e^{-\frac{i\Omega}{2}\left(\frac{z}{v_0}+\frac{z}{c}\right)} e^{-i(\omega-\omega_0)\frac{\Omega}{u}}\, e^{-\frac{\sigma_\omega^2\Omega^2}{2u^2}}. \tag{2.13}$$

The range of spectral coherence is given by

$$\Omega_{coh}=\int d\Omega\left|\frac{\left\langle \tilde{E}\left(z,\omega-\frac{\Omega}{2}\right)\tilde{E}^*\left(z,\omega+\frac{\Omega}{2}\right)\right\rangle}{\left\langle\left|\tilde{E}(z,\omega)\right|^2\right\rangle}\right|^2=\int d\Omega\, e^{-\sigma_\omega^2\Omega^2/u^2}=\frac{\sqrt{\pi}\,|u|}{\sigma_\omega}=|u|\tau_{coh}. \tag{2.14}$$

In the absence of the frequency chirp, $\Omega_{coh}=2\pi/T_b$. In this paper, when we consider a chirped electron beam, we assume $|u|\tau_{coh}>>\frac{2\pi}{T_b}$.

The Wigner function[11] is defined by

$$W(z;t,\omega)=\int d\tau\left\langle E\left(z,t-\frac{\tau}{2}\right)E^{*}\left(z,t+\frac{\tau}{2}\right)\right\rangle e^{-i\omega\tau}\ . \tag{2.15}$$

It can be thought of as analogous to a phase space density (Fig.4) of the radiation and one can easily show that

$$\int\frac{d\omega}{2\pi}W(z;t,\omega)=\left\langle\left|E(z,t)\right|^{2}\right\rangle \tag{2.16}$$

and

$$\int dt\,W(z;t,\omega)=\left\langle\left|\tilde{E}(z,\omega)\right|^{2}\right\rangle. \tag{2.17}$$

From Eqs. (2.10) and (2.15) one finds

$$W(z;t,\omega)\propto e^{2\rho\sqrt{3}k_{w}z}\exp\left(-\frac{\left[\omega-\omega_{0}-u\left(t-\frac{1}{2}\left(\frac{z}{v_{0}}+\frac{z}{c}\right)\right)\right]^{2}}{2\,\sigma_{\omega}^{2}}\right). \tag{2.18}$$

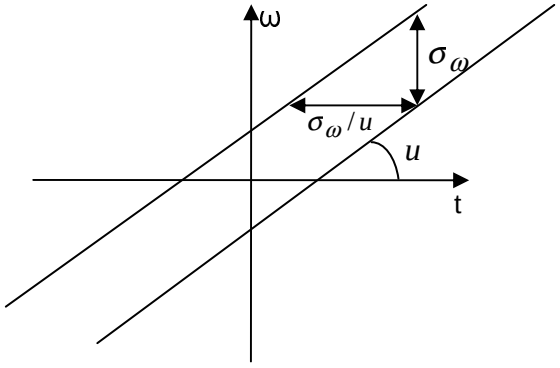

Fig. 4. Time-frequency phase space for chirped radiation.

The following intuitive picture has emerged. Before chirping the electron beam, the radiation occupies a phase space area $\sigma_\omega T_b$. Introducing an electron energy chirp results in a frequency chirp of the radiation, but leaves the phase space area unchanged, still equal to $\sigma_\omega T_b$. The number of modes M [8,9] in a radiation pulse is given by

$$M \equiv \frac{T_b}{\tau_{coh}} = \frac{\sigma_\omega T_b}{\sqrt{\pi}}, \tag{2.19}$$

independent of the energy chirp. For the unchirped electron beam,

$$M = \frac{2\sqrt{\pi}\sigma_\omega}{\Omega_{coh}} = \frac{2\sqrt{\pi}\sigma_\omega}{2\pi / T_b}. \tag{2.20}$$

In the case of the chirped electron beam, the width of the frequency distribution is uT_b, and one can write

$$M = \frac{|u|T_b}{\Omega_{coh}} = \frac{uT_b}{\sqrt{\pi}\, u/\sigma_\omega}. \tag{2.21}$$

III. PULSE SLICING USING A MONOCHROMATOR

One can use a monochromator to select a short portion of the frequency chirped radiation pulse. In order to investigate the properties of such filtered output, let us assume that the electric field $E_F(t,z)$ after the monochromator has the form

$$E_F(z,t) = \int \frac{d\omega}{2\pi} e^{-i\omega t}\, \tilde{E}(z,\omega) e^{-\frac{(\omega-\omega_m)^2}{4\sigma_m^2}}, \tag{3.1}$$

where $\tilde{E}(\omega,z)$ is the Fourier component of the electric field before the filter. The temporal profile of the intensity after the monochromator can be found in terms of the frequency correlation function from the relation

$$\begin{aligned}&\langle E_F(z,t) E_F^*(z,t+\tau)\rangle \\ &= \int \frac{d\omega}{2\pi} e^{-i\omega t} e^{-\frac{(\omega-\omega_m)^2}{4\sigma_m^2}} \int \frac{d\Omega}{2\pi} e^{i(\omega+\Omega)(t+\tau)} e^{-\frac{(\omega+\Omega-\omega_m)^2}{4\sigma_m^2}} \left\langle \tilde{E}(z,\omega)\tilde{E}^*(z,\omega+\Omega)\right\rangle\end{aligned} \tag{3.2}$$

Using Eqs. (2.13) and (3.2), we find

$$\left\langle \left|E_F(z,t)\right|^2 \right\rangle \propto e^{2\rho\sqrt{3}k_w z} \exp\left(-\frac{(t-t_m(z))^2}{2\sigma_t^2} \right), \tag{3.3}$$

where

$$t_m(z) = \frac{\omega_m - \omega_0}{u} + \frac{1}{2}\left(\frac{z}{v_0} + \frac{z}{c} \right). \tag{3.4}$$

The pulse duration is characterized by the rms width σ_t given by

$$\sigma_t^2 = \frac{\sigma_\omega^2 + \sigma_m^2}{u^2} + \frac{1}{4\sigma_m^2}. \tag{3.5}$$

From Eq. (3.5), it is seen that the pulse duration cannot be made smaller than σ_ω / u, which is also apparent from the phase space geometry shown in Fig. 4. The last term in Eq. (3.5) assures that the filtered pulse cannot be shorter than the Fourier transform limit. The minimum pulse duration is obtained for monochromator bandwidth

$$\frac{\sigma_m}{\omega_0} = \sqrt{\frac{|u|}{2\omega_0^2}}. \tag{3.6}$$

This corresponds to a minimum rms pulse duration,

$$(\sigma_t)_{\min} = \sqrt{\frac{\sigma_\omega^2 + |u|}{u^2}}. \tag{3.7}$$

The fractional shot-to-shot energy fluctuation σ_W / W after the monochromator can be expressed in the form [9]

$$\frac{\sigma_W^2}{W^2} = \frac{\int d\omega d\omega' \left\langle \left|\tilde{E}_F(z,\omega)\right|^2 \right\rangle \left\langle \left|\tilde{E}_F(z,\omega')\right|^2 \right\rangle |g_1(z,\omega,\omega')|^2}{\int d\omega \left\langle \left|\tilde{E}_F(z,\omega)\right|^2 \right\rangle \int d\omega' \left\langle \left|\tilde{E}_F(z,\omega')\right|^2 \right\rangle}, \tag{3.8}$$

where

$$|g_1(z,\omega,\omega')| = \frac{\left|\left\langle \tilde{E}_F(z,\omega)\tilde{E}_F{}^*(z,\omega')\right\rangle\right|}{\sqrt{\left\langle\left|\tilde{E}_F(z,\omega)\right|^2\right\rangle\left\langle\left|\tilde{E}_F(z,\omega')\right|^2\right\rangle}} = e^{-\frac{\sigma_\omega^2(\omega-\omega')^2}{u^2}} . \quad (3.9)$$

The second equality in Eq. (3.9) follows from Eq. (2.13)and (3.1). We also know that

$$\left\langle\left|\tilde{E}_F(z,\omega)\right|^2\right\rangle \propto e^{-\frac{(\omega-\omega_m)^2}{2\sigma_m^2}} . \quad (3.10)$$

Inserting Eqs. (3.9) and (3.10) into Eq. (3.8), we find

$$\frac{\sigma_W^2}{W^2} = \frac{|u|}{\sqrt{u^2+4\sigma_m^2\,\sigma_\omega^2}} \equiv \frac{1}{M_F}, \quad (3.11)$$

where

$$M_F = \sqrt{\frac{4\sigma_m^2\sigma_\omega^2}{u^2}+1} \quad (3.12)$$

is the number of modes in the pulse after the monochromator.

The time-correlation function of the filtered radiation can be calculated using Eq. (3.2), and one finds

$$\left\langle E_F\left(z,t-\frac{\tau}{2}\right)E_F{}^*\left(z,t+\frac{\tau}{2}\right)\right\rangle \propto e^{2\rho\sqrt{3}k_w z}e^{i\omega_m\tau}e^{-\frac{\sigma_m^2\tau^2}{2}}e^{-\frac{\left(t-t_m(z)-i\frac{\sigma_m^2\tau}{u}\right)^2}{2\sigma_t^2}} . \quad (3.13)$$

The coherence time of the radiation after the monochromator is

$$\tau_{coh} = \int d\tau \left|\frac{\left\langle E_F\left(z,t-\frac{\tau}{2}\right)E_F{}^*\left(z,t+\frac{\tau}{2}\right)\right\rangle}{\left\langle E_F(z,t)E_F{}^*(z,t)\right\rangle}\right|^2 = \frac{2\sqrt{\pi}\,\sigma_t}{M_F} . \quad (3.14)$$

IV. SHORT X-RAY PULSES AT THE LCLS

We consider the linac coherent light source (LCLS) [1] under design at SLAC. The fundamental wavelength of this SASE FEL is 1.5 $\overset{o}{A}$ corresponding to $\omega_0 = 1.2\times10^{19}\, s^{-1}$. The SASE bandwidth near saturation is approximately given by $\sigma_\omega / \omega_0 \cong \rho \cong 5\times10^{-4}$. The electron bunch has a FWHM duration of $T_b = 230\, fs$. A one-percent energy chirp across the electron bunch, $\alpha = .01$, corresponds to a frequency chirp $u = \Delta\omega/\Delta t = 7\times10^{-9}\omega_0^2$. The coherence time $\tau_{coh} = \sqrt{\pi}/\sigma_\omega = .3\, fs$ and the range of spectral coherence $\Omega_{coh} = u\tau_{coh} = 2.5\times10^{-5}\omega_0 = 6\times10^{-2}\sigma_\omega$.

From Eq. (3.6), we see that the minimum pulse duration is obtained for monochromator bandwidth

$$\frac{\sigma_m}{\omega_0} = \sqrt{\frac{|u|}{2\omega_0^2}} = 6\times10^{-5}. \tag{4.1}$$

Using Eq. (3.7) and the fact that $|u| << \sigma_\omega^2$, the corresponding minimum rms pulse duration is found to be

$$(\sigma_t)_{\min} \cong \frac{\sigma_\omega}{|u|} = 6\, fs. \tag{4.2}$$

The temporal coherence time near the minimum pulse length is [from Eq. (3.14)]

$$\tau_{coh} \cong \frac{\sqrt{\pi}}{\sigma_m} = 2.5\, fs\ , \tag{4.3}$$

and the spectral coherence range is unchanged by using the monochromator,

$$\Omega_{coh} = \frac{\sqrt{\pi}\,|u|}{\sigma_\omega} \cong \frac{\sqrt{\pi}}{\sigma_t}. \tag{4.4}$$

The number of modes at the minimum pulse duration is

$$M_F = \frac{2\sqrt{\pi}\,\sigma_t}{\tau_{coh}} \cong \frac{2\sigma_m\sigma_\omega}{|u|} = 9, \tag{4.5}$$

corresponding to a fractional energy fluctuation

$$\frac{\sigma_W}{W} = \frac{1}{\sqrt{M_F}} = 33\%. \tag{4.6}$$

As seen in Fig. 5, the minimum of σ_t as a function of σ_m is broad, so it is feasible to choose the monochromator bandwidth larger than the optimum value in order to increase the number of modes M_F and thus decrease the pulse energy fluctuation σ_W / W.

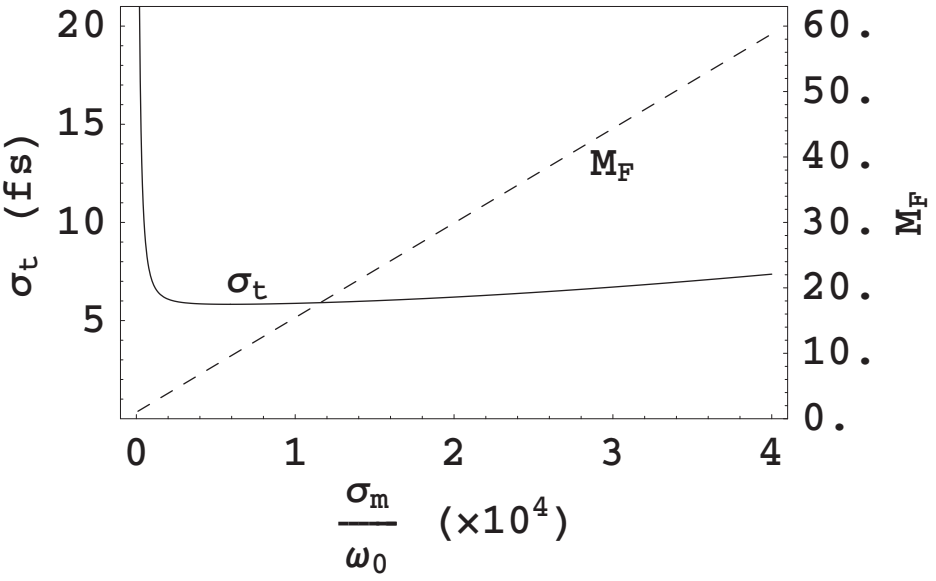

Fig. 5. For LCLS, we plot the rms pulse duration σ_t and the number of modes M_F of the radiation after a monochromator with rms bandpass σ_m / ω_0 for a (full) energy chirp of 1%. The SASE gain bandwidth is taken to be $\sigma_\omega / \omega_0 = 5 \times 10^{-4}$, which is the value (equal to the Pierce parameter) expected near saturation.

V. SUMMARY AND DISCUSSION

We have carried out a statistical analysis of the temporal and spectral properties of SASE from an energy-chirped electron beam passing through a long undulator, characterizing the radiation both before and after a monochromator used to select a short duration slice of the radiation pulse. In our study, we have considered the number of modes M in the radiation using the definition found in Goodman [8]. That is, the number of modes is defined in terms of the pulse energy fluctuation $M \equiv \frac{W^2}{\sigma_W^2}$. If T_b is the (full) duration of the pulse having step function profile, then Goodman defines the coherence time by

$\tau_{coh} \equiv \frac{T_b}{M}$. Another quantity of interest is the number of spikes observed in the SASE output. In ref. [10], it was shown that for unchirped SASE the number of temporal spikes is $N_s \cong 0.711M$, where following Rice [14], the temporal spikes were characterized by the existence of local maxima of the intensity. If we define the full spectral width to be $\Delta\omega \equiv 2\sqrt{\pi}\sigma_\omega$ then the number of spectral peaks is [10] $0.641M$.

A summary of some of our results is given in Table 1. In this table the filtered quantities are evaluated near the pulse length minimum, when $\sigma_m \approx \sqrt{\frac{|u|}{2}} << \sigma_\omega$. Also, whenever the temporal or spectral distribution is Gaussian with rms deviation σ, we choose the "full width" to be $2\sqrt{\pi}\sigma$.

Table 1. Properties of Unchirped, Chirped and Filtered SASE

	Unchirped	Chirped	Filtered
Pulse duration	T_b	T_b	$2\sqrt{\pi}\sigma_\omega/\|u\|$
Coherence time	$\sqrt{\pi}/\sigma_\omega$	$\sqrt{\pi}/\sigma_\omega$	$\sqrt{\pi}/\sigma_m$
Number of modes	$T_b\sigma_\omega/\sqrt{\pi}$	$T_b\sigma_\omega/\sqrt{\pi}$	$2\sigma_m\sigma_\omega/\|u\|$
Spectral width	$2\sqrt{\pi}\sigma_\omega$	$\|u\|T_b$	$2\sqrt{\pi}\sigma_m$
Spectral coherence range	$2\pi/T_b$	$\sqrt{\pi}\|u\|/\sigma_\omega$	$\sqrt{\pi}\|u\|/\sigma_\omega$

As seen from Eq. (1.1), the minimum pulse duration after the monochromator cannot be less than $\sigma_\omega/|u|$. Since $\sigma_\omega \propto \frac{1}{\sqrt{z}}$, shorter pulse duration is achievable for larger z (before saturation). This has implications for the optimization of the two-stage approach. Moreover, inclusion of three-dimensional effects may be important to obtain accurate estimates for the SASE bandwidth and hence the minimum achievable pulse length.

ACKNOWLEDGEMENTS

Z.H. wishes to thank E. Saldin and S. Reiche for stimulating discussions on the monochromatization of chirped SASE. This work was supported by Department of Energy contracts DE–AC03–76SF00515 and DE-AC02-98CH10886.

REFERENCES

[1] J. Galayda, ed., *Linac Coherent Light Source Conceptual Design Report*, SLAC-R-593 (2002).

[2] G.T. Moore, Nucl. Instrum. Meth. **A272**, 302 (1988).

[3] L.H. Yu, E. Johnson, D. Li, D. Umstadter, Phys. Rev. **E49**, 4480 (1994).

[4] C. Pellegrini, Nucl. Instrum. Meth. **A445**, 124 (2000).

[5] C.B. Schroeder, C. Pellegrini, S. Reiche, J. Arthur and P. Emma, Nucl. Instrum. Meth. **A483**, 89 (2002).

[6] *C*.B. Schroeder, C. Pellegrini, S. Reiche, J. Arthur and P. Emma, J. Opt. Soc. Am. **B19** (2002).

[7] Y.L. Li, J. Lewellen, Z. Huang, V. Sajaev and S. Milton, Phys. Rev. Lett. **89**, 234801-1 (2002).

[8] J.W. Goodman, *Statistical Optics*, John Wiley & Sons, New York (1985).

[9] E.L. Saldin, E.A. Schneidmiller, M.V. Yurkov, *The Physics of Free Electron Lasers*, Springer-Verlag, Berlin (2000).

[10] S. Krinsky and R.L. Gluckstern, Nucl. Instrum. Meth. **A483**, 57 (2002).

[11] K.J. Kim, "Characteristics of Synchrotron Radiation" in *Proceedings U.S. Particle Accelerator School*-1987, edited by M. Month et al, AIP Conference Proceedings 184, New York: American Institute of Physics, 1989, pp. 565-632.

[12] S.O Rice, Bell System Technical Journal **24** (1945) 46.

[13] K.J. Kim, Nucl. Instrum. Meth. **A250**, 396 (1986).

[14] J.M. Wang and L.H. Yu, Nucl. Instrum. Meth. **A250**, 484 (1986).

Appendix A: VLASOV-MAXWELL EQUATIONS

We shall now derive the approximate expression for the green's function presented in Eq. (2.7). The radiated electric field E is expressed in terms of the slowly varying amplitude A according to $E = A\exp(ik_0 z - \omega_0 t)$. We introduce the dimensionless variables $Z = k_w z$, $\theta = (k_0 + k_w)z - \omega_0 t$, and $p = 2(\gamma - \gamma_0)/\gamma_0$, and the electron distribution function $\psi(\theta, p, Z)$. The one-dimensional, linearized Vlasov-Maxwell equations are [13,14]

$$\frac{\partial \psi}{\partial Z} + p\frac{\partial \psi}{\partial \theta} - \frac{2D_2}{\gamma_0^2}\left(Ae^{i\theta} + A^* e^{-i\theta}\right)\frac{\partial \psi_0}{\partial p} = 0, \tag{A1}$$

$$\left(\frac{\partial}{\partial Z} + \frac{\partial}{\partial \theta}\right)A = \frac{D_1}{\gamma_0}e^{-i\theta}\int dp\,\psi(\theta, p, Z), \tag{A2}$$

with (mks units)

$$D_1 = \frac{ea_w n_0 [JJ]}{2\sqrt{2}\,k_w \varepsilon_0} \quad \text{and} \quad D_2 = \frac{ea_w [JJ]}{\sqrt{2}\,k_w mc^2}. \tag{A3}$$

n_0 is the electron beam density and $[JJ] = J_0\left(\frac{a_w^2}{2(1+a_w^2)}\right) - J_1\left(\frac{a_w^2}{2(1+a_w^2)}\right)$. The equilibrium distribution of the chirped electron beam is taken to be

$$\psi_0 = \delta(p + \mu\theta_0), \tag{A4}$$

where

$$\theta_0 = \theta - pZ \text{ and } \mu = u/\omega_0^2 . \tag{A5}$$

We can solve the Vlasov equation (A1) for the distribution in terms of the field and insert the result in the Maxwell equation (A2) to obtain the dispersion relation [6]. Assuming $\mu Z << 1$, we derive

$$\left(\frac{\partial}{\partial Z} + \frac{\partial}{\partial \theta}\right)A \cong \frac{D_1}{\gamma_0}\sum_j e^{-i\theta_j + i\mu Z\theta_j}\delta(\theta - \theta_j) + i(2\rho)^3\int_0^Z dZ'(Z - Z')\,A(\theta, Z')e^{i\mu(Z-Z')\theta}, \tag{A6}$$

where $\theta_j = -\omega_0 t_j$ and $(2\rho)^3 = \frac{2D_1 D_2}{\gamma_0^3}$. This equation can be solved by Laplace transform. We define

$$f(\theta, s) = \int_0^\infty dZ\ e^{-sZ} A(\theta, Z). \tag{A7}$$

Then Eq. (A6) reduces to the following ordinary differential equation

$$\frac{\partial f}{\partial \theta} + \left[s - \frac{i(2\rho)^3}{(s - i\mu\theta)^2} \right] f = A(\theta,0) + \frac{D_1}{\gamma_0} \sum_j \frac{e^{-i\theta_j}\, \delta(\theta - \theta_j)}{s - i\mu\theta_j}, \tag{A8}$$

whose solution is

$$f(\theta, s) = \int_{-\infty}^{\theta} d\theta'\ \exp\left(-s(\theta - \theta') + \frac{i(2\rho)^3(\theta - \theta')}{(s - i\mu\theta)(s - i\mu\theta')} \right) \left[A(\theta',0) + \frac{D_1}{\gamma_0} \sum_j \frac{e^{-i\theta_j}\, \delta(\theta' - \theta_j)}{s - i\mu\theta_j} \right] \tag{A9}$$

The field is then determined from the inverse Laplace transform

$$A(\theta, Z) = \int_C \frac{ds}{2\pi i}\, e^{sZ}\ f(\theta, s). \tag{A10}$$

We restrict our attention to the case of SASE and take $A(\theta,0) = 0$. Then one can derive

$$A(\theta, Z) = \frac{D_1}{\gamma_0} \sum_j e^{-i\theta_j} H(\theta - \theta_j) \int_C \frac{ds}{2\pi i s}\, e^{(s + i\mu\theta_j)(Z - \theta + \theta_j)}\, e^{\frac{i(2\rho)^3(\theta - \theta_j)}{s(s - i\mu(\theta - \theta_j))}}, \tag{A11}$$

where $H(\theta)$ is the Heaviside step function equal to 1 for $\theta > 0$ and to 0 for $\theta < 0$. It then follows that

$$\begin{aligned} E &= A\, e^{i(\theta - Z)} \\ &= \frac{D_1}{\gamma_0} \sum_j e^{i(1 - \mu\theta_j)(\theta - Z - \theta_j)} g(Z, \theta - \theta_j; \mu) \\ &= \frac{D_1}{\gamma_0} \sum_j e^{i[k_j z - \omega_j (t - t_j)]} g(Z, \theta - \theta_j; \mu) \end{aligned} \tag{A12}$$

where

$$g(Z,\theta;\mu)=H(\theta)\int_C \frac{ds}{2\pi i s}\exp\left(s(Z-\theta)+\frac{i(2\rho)^3\theta}{s(s-i\mu\theta)}\right). \qquad \text{(A13)}$$

We estimate the contour integral in Eq. (A13) by a saddle point approximation. The saddle point is determined as a power series in μ. Keeping only the linear term we find

$$g(Z,\theta;\mu)\cong e^{\rho(\sqrt{3}+i)Z}e^{-\rho(\sqrt{3}+i)\frac{9(\theta-Z/3)^2}{4Z}}e^{\frac{i\mu}{2}(Z-\theta)\theta}. \qquad \text{(A14)}$$

We are ignoring the small reduction in gain [5,6] which enters in $O(\mu^2)$. This is the result used in Eq. (2.7).

APPENDIX B. TIME CORRELATION FUNCTION

Consider the electric field to be determined by Eqs. (2.6) and (2.7), with $\omega_j=\omega_0+ut_j$. We average over the independent random variables t_j and use $\left\langle e^{iat_j}\right\rangle=0$ to derive

$$\left\langle E(z,t)E^*(z,t+\tau)\right\rangle\propto$$
$$e^{2\rho\sqrt{3}k_w z}e^{i(\omega_0+ut)\tau}e^{-\left(b^*-i\frac{u}{2}\right)\tau^2}e^{-\frac{iu}{2}\left(\frac{z}{v_0}+\frac{z}{c}\right)\tau}\sum_j e^{-(b+b^*)\left(t-t_j-\frac{z}{v_g}\right)^2}e^{-2b^*\tau\left(t-t_j-\frac{z}{v_g}\right)} \qquad \text{(B1)}$$

Replacing the sum by an integral over t_j, we find

$$\left\langle E(z,t)E^*(z,t+\tau)\right\rangle\propto e^{2\rho\sqrt{3}k_w z}e^{\frac{-iu\tau}{2}\left(\frac{z}{v_0}+\frac{z}{c}\right)}e^{i\left(\omega_0+u\left(t+\frac{\tau}{2}\right)\right)\tau}e^{-\frac{\sigma_\omega^2\tau^2}{2}}. \qquad \text{(B2)}$$

The result of Eq. (2.10) follows immediately.